A general approach to discover conformational epitope-directed binders for selective inhibition of protein proteolytic activation

Authors: Jie Zhou[1], Katlin Schaefer[1], Soumya G. Remesh[1], Kevin K. Leung[1], James A. Wells[1,2,3,#]

Affiliations

[1]Department of Pharmaceutical Chemistry, University of California San Francisco, San Francisco, CA, 94158, USA.

[2]Chan Zuckerberg Biohub; San Francisco, CA, 94158, USA.

[3]Department of Cellular and Molecular Pharmacology, University of California San Francisco, San Francisco, CA, 94158, USA.

#Corresponding Author. Email: jim.wells@ucsf.edu

Abstract

The generation of antibody that binds to a specific conformational epitope of a target protein remains an outstanding challenge. We describe here a general approach to select and identify epitope-directed antibodies using a differential phage selection strategy. Prior to positive selection against protein of interest (POI), any binders that bind to undesired epitopes are depleted from the Fab phage library by a POI mutant with epitope of interest (EOI) mutated or blocked. As a proof-of-concept, we successfully developed highly specific antibodies targeting the proteolytic site on the CUB domain containing protein 1 (CDCP1) to block its proteolysis. We also generated antibodies recognizing the junction between the prodomain and catalytic domain of Matrix Metalloprotease 9 (MMP9) to block its maturation. Different from traditional MMP inhibitors targeting catalytic site, these potent MMP9 inhibitory antibodies are a novel class of MMP inhibitors with improved selectivity and stability. The inhibiting mechanism is unique among inhibitory antibodies and represents a new approach for developing molecules that inhibit therapeutic targets. These antibodies have shown promise in blocking metastasis of an invasive breast cancer cell line and are invaluable tools to assist the identification of MMP9 substrates by proteomics. We demonstrated the generality and versability of this approach by developing binders that block proteolytic activation of diverse protein targets with very distinct shapes and biological roles, including three MMPs (i.e., MMP1, MMP3, MMP10) and a cell surface receptor EPH Receptor A2 (EphA2). Our approach enables the generation of binders to the sites of interest on a wide variety of proteins for broad therapeutic and diagnostic applications.

Introduction

Over the past two decades, therapeutic antibodies have become the leading products within the biopharmaceutical market.[1] These antibodies often require binding to a specific epitope on a protein target to exert their functions, e.g., blocking a ligand-receptor interaction[2,3], eliciting agonistic activities on receptors[4], and stabilizing protein complex[1]. Although mouse immunization[5] and phage/yeast display technologies[6,7] are routinely used to generate antibodies with high affinity and specificity. The epitope dependence exerts a great challenge to the current antibody generation pipeline. Typically, one has to screen hundreds of hits from phage panning or hybridoma clones generated from mouse immunization to hopefully identify the antibodies binding to the desired epitopes. Although mouse immunization with linear peptide containing epitope of interest (EOI) leads to antibodies recognizing that desired epitope, these antibodies do not necessarily bind to the EOI in a 3D conformation. There is a lack of simple approach to generate epitope-directed binders to an EOI on a target protein.

Very recently, Wang group has developed a method to allow epitope-directed antibody generation using phage panning technology coupled with photo-crosslinking enabled by the incorporation of a noncanonical photoreactive amino acid into the EOI.[8] However, this method is time- and effort-consuming, only works for proteins and expression systems allowing noncanonical amino acid incorporation while not disrupting protein tertiary folding, and often generates non-specific binders. Differential phage selection is a powerful strategy to obtain highly specific antibodies for specific protein conformations[9], isoforms[10], and even small molecule complexes[11]. Inspired by this, we developed a more general approach to select and identify epitope-directed antibodies by deploying differential phage selection (**Fig. 1a**). In brief, prior to positive selection against wild type (wt) protein of interest (POI), any binders that bind to undesired epitopes are stringently depleted from the Fab phage library by a POI mutant with EOI mutated or blocked. After 3-4 rounds of iterative selections, only Fab phage recognizing the EOI with good affinity would be enriched for further validation. A systematic bioinformatics analysis revealed that antibody binding involves more residues in loops than helixes and sheets, and certain amino acids favors antibodies recognition while other not. This information guides the design of mutants used for library clearance.

Extracellular proteolysis has major functional consequences for remodeling cell surface proteins and the extracellular matrix (ECM).[12-14] Alterations in proteolytic systems underlie multiple pathological conditions, including neurodegenerative disorders[15,16], inflammatory diseases[17], and cancers[18,19]. Blocking pericellular proteolysis will provide insights into proteolysis-regulated

cellular activity, its role in disease, and potential therapeutic opportunities. The approach we have developed provide a great chance for us to precisely regulate the proteolysis of cell surface receptors (e.g., CDCP1, EphA2) and the proteolytic activation of pro-enzyme (MM1, MMP3, MMP9 and MMP10). This approach will allow the generation of binders to the sites of interest on a wide variety of proteins for broad therapeutic and diagnostic applications.

Result

Structural bioinformatics guides the design of mutants used for negative selections

We first sought to determine the prevalence of different secondary structures adopted by the residues on an antigen involved in antibody recognition. We downloaded ~1200 structures of antigen-antibody (in Fv format) complexes from AbDb[20], a database which collects the Fv regions from antibody structure in complex with its antigen from Protein Data Bank (PDB). A distance cutoff of 3Å allows a robust identification of residues in the antibody-antigen interface. Using the standard Dictionary of Secondary Structure of Proteins (DSSP) algorithm[21], we calculated the secondary structures of all the residues within the 3Å distance cutoff (**Fig. 1b, 1c**). We found that 60% of the residues in the epitopes adopted loop structure, while Helix or Sheet occurred only 20% of the time, respectively. This analysis revealed that antibody binding involves more residues in loops than helixes and sheets on an antigen. This is not surprising since the flexibility of loop make it easy to interact with the six hypervariable antibody complementarity-determining region (CDR) loops. This is appealing since making mutations on loop has minimum disruption on protein folding. We then analyzed the abundancy for each of the 20 amino acids of the residues on the antigens interacting with CDRs on antibodies and compared this with natural amino acid abundancy (**Fig. 1d**). Obviously, certain amino acids (e.g., Asn, Arg, Asp, Trp, Tyr, etc) with side chains that could provide strong electrostatic interaction or pi-pi stacking, are favored, while others like Ala, Leu, Val, which need to cluster to exhibit strong interactions, are not favored. This information provides valuable guidance for the design of mutants used for negative selection: 1) the favored residues should be mutated to very distinct amino acids; 2) residues could be mutated to unfavored amino acids or those with small side chain (like Ala, Ser or Gly); 3) prioritize making mutation on unstructured regions.

Proof-of-concept: generation of site-directed antibody blocking CDCP1 proteolysis

CDCP1 is a Type I single-pass membrane protein that is highly overexpressed in a variety of solid tumors.[22,23] It is proteolytically processed to generate a N-terminal and C-terminal fragment (NTF and CTF, respectively). We previously identified a nested set of three cleave sites with four basic

amino acids of each other between the NTF and CTF and validated that the NTF stay tightly associated upon proteolysis (**Fig. 2a**).[10] Using CDCP1 as a model system, we aimed to generate antibodies specifically targeting the proteolytic sites (R415-K420) to block its proteolysis.

First, we engineered antigens for differential selection by grafting the extracellular domain (ECD) of CDCP1 onto a Fc owning a C-terminal avi-tag for biotinylation. A TEV cleavage site was incorporated right before the hinge region in Fc for phage elution (**Fig. 2a, Extended Data Fig. 1a**). Two mutants of CDCP1-Fc were generated by mutating the residues surrounding the proteolytic sides: RK(418-419) -> AA and VKQSRK(414-419) -> GGSGGS. Two phage selection campaigns were conducted with each of the two mutants. To generate an antibody that can specifically recognize the EOI, we employed the differential phage selection strategy using an in-house Fab phage library (**Fig. 2b**). Prior to each round of selection, the phage pool was cleared with the mutant (CDCP1-$Fc^{mutant1/2}$) before positive selection with CDCP1-Fc^{wt}. The first-round clearance used Fc domain only in order to keep a high sequence diversity in the initial state. After 3-4 rounds of iterative selection, there was enrichment for Fab phage that bound CDCP1-Fc^{wt} over CDCP1-$Fc^{mutant1/2}$. The enrichment was characterized by phage titer as a function of round of selection (**Extended Data Fig. 1b**). Since the only difference between the negative and positive selection antigens are the EOI, we expected the enriched Fab phage to exclusively bind to the EOI.

For each of the two selections, we characterized the binding of 96 phage clones to the CDCP1-Fc^{wt} and CDCP1-$Fc^{mutant1/2}$ by phage ELISA (**Fig. 2c, Extended Data Fig. 1c, 1d**). A group of Fab phage clones were identified to preferentially bind to the wt antigen over the mutants. The unique Fab phage clones (**Fab. 2d**) were recombinantly expressed as Fabs or IgGs for further characterization. A biolayer interferometry（BLI) experiment revealed that all the three antibodies selective bind to uncleaved CDCP-Fc^{wt} (Kd ~ 8 nM for IgG 0151, 6 nM for IgG 0152, and 4 nM for IgG 0153) with minimum binding to three cleaved CDCP1 isoforms (**Fig. 2e, Extended Data Fig. 2**). Our previous study indicated that cleaved and uncleaved CDCP1 have almost identical conformations since NTF stay attached (**Fig. 2a**).[10] This supported that the three binders selectively binds to the proteolytic sites of CDCP1. IgG 0151, from the selection campaign using CDCP1-$Fc^{mutant1}$ for negative selection, exhibits minimum binding to both mutants, while from selection using CDCP1-$Fc^{mutant2}$ for negative selection, IgG 0152 recognizes CDCP1-$Fc^{mutant1}$ with impaired affinity (Kd ~15 nM) and does not bind to CDCP1-$Fc^{mutant2}$, and IgG 0153 partially binds to both mutants (Kd ~5 nM for CDCP1-$Fc^{mutant1}$ and 6 nM for CDCP1-$Fc^{mutant1}$). This indicates that R418 and K419 were required for IgG 0151 binding but not for IgG 0152 binding. IgG 0152

involves KQS(415-417) for binding while for IgG 0153, KQSRK site plays a role but very little in antibody binding. Agree with this, an epitope binning by a sequential BLI experiment indicates that the epitopes for all three IgGs are slightly different (**Fig. 2f**). These results inform that by controlling the size of the mutation site, we can control the specificity of the resulting binders.

Plasmin is reported to be one of the proteases that can cleave CDCP1.[24] We found that plasmin mediated CDCP1 proteolysis can be efficiently blocked by the three antibodies (**Fig. 2g, 2h**). Specifically, 0.5 μg/μL plasmin cleaved 70% of CDCP1-Fc within 1 hour while in the presence of each of the three antibodies, less 10% would be cleaved.

Generating side-directed antibody to block MMP9 maturation

MMP9 plays a pathological role in a variety of inflammatory and oncology disorders and has long been considered an attractive therapeutic target.[25] Latency of MMP9 (i.e., proMMP9) is maintained by an electrostatic interaction between the free thiol of a conserved cysteine in the prodomain with the His-ligated zinc atom in the catalytic pocket. Proteolytic cleavage of the prodomain by other proteases removes the thiol constraint. The activation of MMP9 can also be initiated by autolysis if the interaction between prodomain and catalytic core is disrupted by nonproteolytic means such as 4-Aminophenylmercuric acetate (APMA), Sodium dodecyl sulfate (SDS), or protein-protein interaction (**Fig. 3a**)[26]. Here we wanted to generate site-directed antibody recognizing the junction between the prodomain and catalytic domain (**Fig. 3b**) to block MMP9 activation as a novel class of MMP9 inhibitor.

We first expressed antigens for phage selection by generating a truncated form of MMP9 fused to Fc (MMP9-pro-cat-Fc^{wt}) containing an internal deletion of the fibronectin type II-like domain (Fn) and a C-terminal deletion of the hemopexin domain (Hpx). The residues around the proteolytic activation site (R106/F107) as the EOI was mutated to generate negative selection antigens MMP9-pro-cat-Fc$^{mutant1/2}$ (**Fig. 3c, 3d, 3e, Extended Data Fig. 3a**). Using INPS-MD, a web server to predict stability of protein variants from sequence and structure[27], we calculated the ΔΔG values of individual mutation to make sure the protein stability won't be disrupted by these mutations (**Fig. 3e**).

We then conducted the same phage selection campaign as we did for CDCP1 and observed a significant enrichment for wt antigen over mutants (**Extended Data Fig. 3b**). Phage ELISA on 96 clones from each selection campaign followed by Sanger sequencing identified seven out of nine unique Fab clones that preferentially bind to the wt antigen over at least one of the mutants (**Fig. 3f, Extended Data Fig. 3c**). BLI experiments confirmed the selective binding of these clones after

being expressed in Fab format (**Fig. 3g, Extended Data Fig. 4**). We also expressed and purified this truncated antigen with His-tag (MMP9-pro-cat-His^{wt}, **Extended Data Fig. 5**) in E coli inclusion bodies and confirmed the comparable binding of these seven Fabs to this antigen using BLI (**Fig. 3g**).

Antibodies binding junction region between prodomain and catalytic domain block MMP9 maturation

To determine whether the Fabs could inhibit pro-MMP9 activation, we checked the activation of pro-MMP9 (G100L) overexpressed from a stable HEK293T cell line in the presence of these Fabs by western blot. The weakened interaction between the prodomain and the catalytic domain of pro-MMP9 (G100L) leads to increased activation of MMP9 in the cell culture.[28] According to the western blot of MMP9 in conditioned medium and the corresponding quantification (**Fig. 3h, 3i**), Fab 155, 156, 157, 159, 160, 166 and 167 caused a significant decrease (~ 50%) in the amount of active MMP9 compared with Fab 162 and 163, that bind MMP9 but not the junction region and the control Fab. This result confirmed that these Fabs that recognize proteolytic activation site on MMP9 could inhibit MMP9 proteolytic activation.

Para-Methoxyamphetamine (PMA)[29] is reported to upregulate MMP9 expression in MCF-7, a breast cancer cell line. Indeed, PMA treatment caused an increase in proMMP9 expression but not active MMP9 (**Fig. 3j**). APMA promotes MMP9 activation through autolysis by breaking the interaction between prodomain and catalytic domain and causing conformation perturbance (**Fig. 3a, Fig. 3j**). This could also be significantly blocked by Fab157, 166, and 167 as shown in zymography analysis on the conditioned medium (**Fig. 3j, 3k**), indicating that these three Fabs could further block MMP9 maturation by stabilizing the interaction between the prodomain and catalytic domain and preventing autolysis.

MMP9 inhibitory antibodies block cancer invasion

MMP9 is thought to play a key role in tumor invasion and metastasis.[30] We then proceeded to test whether these inhibitory antibodies would slow down metastasis of an invasive breast cancer line HT-1080. After confirming that these inhibitory antibodies block MMP9 maturation in HT-1080 cell culture (**Extended Data Fig. 6a, 6b**), we conducted a Trans-well cell migration assay in the presence of individual antibody versus a nonbinding control antibody. Obviously, the invasion or migration of HT-1080 cells through the Matrigel coated membrane was significantly slowed down by these inhibitory antibodies to different extents (~30-50%) (**Fig. 4a**). Different from traditional MMP inhibitors targeting catalytic sites, we anticipated these antibodies have improved specificity

and stability due to this unique inhibiting mechanisms. We believed that these antibodies are promising therapeutic MMP9 inhibitors for the treatment of cancers implicated by an upregulation of MMP9.

MMP9 inhibitory antibody facilitates substrate identification by proteomics

One of the potential applications of such inhibitory antibody is to facilitate the identification of MMP9 substrates. We first expressed one of the most potent binder (Fab 166) in IgG format (IgG 166) and confirmed its binding to proMMP9 by BLI (**Fig. 4b,** Kd ~ 1nM). N-glycosylation is present on >85% of cell surface proteins[31] and can be exploited to capture the N-glycosylated proteins using a biotin hydrazide enrichment method (CSC)[32]. Next, we utilized a CSC protocol coupled with stable isotope labeling by amino acids (SILAC) to compare the surfaceomes from HEK293T MMP9 (G100L) w/o IgG 166 treatment (**Fig. 4c**). We used the stable cell line overexpressing MMP9 (G100L) for a higher signal. Any surface proteins enriched on the cells treated with IgG 166 could potentially be the MMP9 substrates. A total of 1600 cell surface proteins were identified, and 69 proteins were remarkably enriched on the cells incubated with IgG 166 (**Fig. 4d**, **Extended Data Table 1**). Some known substrates[33] including amyloid-beta precursor protein (APP), integrin β1 precursor (ITGB1), Fibronectin (FN1), metalloproteinase inhibitor 1 (TIMP-1), and some collagen isoforms have been identified in this experiment. A subset of identified proteins including known MMP9 substrates, and some potential substrates is described in **Extended Data Table 1**. The use of protease inhibitory antibodies for substrates identification not only bypasses tedious genetic modification (e.g., gene knockout or knockdown) but also avoids any possible gene perturbance.

Generalizing differential phage selection approach to other protein targets

To demonstrate the generality of this approach, we planned to develop highly selective blockers of the proteolytic activation of another four protein targets with very distinct shapes and biological roles, including three MMPs (i.e., MMP1, MMP3, MMP10) and a cell surface receptor EphA2 (**Fig. 5a-5d**). All these MMPs play a role in multiple cancers and are promising anti-cancer targets (**Extended Data Fig. 7**). However, there is a lack of selective inhibitors for individual MMP, which remains a great challenge to study biological role and functional redundancy of each MMP and the main reason for the limited clinical outcomes. We envisioned that these MMP blocking antibodies would greatly advance the MMP biology and hold great therapeutic potentials. Proteolysis of EphA2 converts itself from a tumor suppressor to an oncoprotein[34]. We thus believed that blocking its proteolysis would facilitate the reversion of invasive cells to a non-invasive epithelial state.

Similarly, we first expressed antigens for phage selection by generating MMP-pro-cat and Fibronectin type-III domain 1 and 2 (where proteolytic site locates) in Fc fusion (MMP1, 3, 10-pro-cat-Fc^{wt}, Fn III-1/2-Fc^{wt}). The residues around the proteolytic activation sites as the EOIs were mutated to generate negative selection antigens (**Extended Data Table 2**). We conducted the same phage selection campaign as we did for CDCP1 and MMP9 and observed a robust enrichment for wt antigen over mutants for all of the four targets (**Extended Data Fig. 8**). Phage ELISA on 96 clones from each selection campaign followed by Sanger sequencing identified several unique Fab clones that preferentially bind to the wt antigens over at least one of the mutants (**Fig. 5e-5h, Extended Data Fig. 9**). BLI experiments confirmed the selective binding of these clones after being expressed in Fab format to positive selection antigens (**Fig. 5i-5l**) with minimum binding to the mutants (**Extended Data Fig. 10**). Finally, we validated that the proteolytic activation of MMP1, 3, and 10 by MMP9 or trypsin could be efficiently inhibited by these antibodies (**Extended Data Fig. 11a, Fig. 5m-5o**). Moreover, the EphA2 blocking antibodies blocked the proteolysis of EphA2 stably overexpressed on HT-1080 cells (**Extended Data Fig. 11b, Fig. 5p**). The signaling study of EphA2 proteolysis blocked by these antibodies will be discussed in another research.

Discussion

We developed a platform for facile selection and identification of antibodies binding to technically any specific epitope on an antigen using differential phage selection strategy. The foundation of this method is to create an “undesired artificial epitope” by mutation or masking to deplete the Fab phage library of any binders that are “off-target”. The mutation would be preferentially made on residues in unstructured regions and to amino acids that are “unfavored” and distinct from original ones as is guided by structure bioinformatics. The generality and versatility of this approach was demonstrated by the successful generation of functional antibodies to defined epitopes on six different protein targets with distinct shapes and biological roles. These antibodies have great potential to be transformed into novel disease therapeutics and are also valuable tools to study protein functions in various signaling pathways.

The differential phage selection strategy has great adaptability and flexibility. First, by decreasing the stringency of negative selection or clearance (e.g., decreasing negative antigen concentration), binders that slightly touch the edge region of the EOI would be enriched. These binders still have the capability to block proteolysis or PPI due to steric hinderance. Second, the sequence diversity of the resulting antibody repertoire would be enhanced by increasing size the mutation sites (i.e., to create a larger “undesired artificial epitope”). A higher sequence diversity

allows downstream hit optimization and candidate selection. Third, this flatform could be advantageous when the target epitope is on a membrane spanning proteins, such as an ion channel or G protein–coupled receptor (GPCR), a clinical importance but challenging therapeutic target class. In such case, on-cell phage panning could be coupled with this differential phage selection to get site-directed antibodies that would inhibit or stimulate the signaling transduction. Fourth, the generation of catalytic site-specific antibody for an enzyme (e.g., MMPs) could be achieved by slightly modifying this protocol. In brief, negative selection with the enzyme bound with any non-specific inhibitors targeting catalytic sites prior to positive selection with apo enzyme would allow of enrichment of binders specifically targeting the catalytic site. Finally, the same principle would be used in other combinatorial selection technologies, including yeast display based antibody generating pipeline.

To summarize, we have developed a general approach to select and identify epitope-directed antibodies to technically any epitope. We demonstrate the generality and versability of this method by developing binders blocking proteolytic activation of a panel of MMPs and two cell surface receptors CDCP1 and EphA2. The theme of this manuscript is inhibition of proteolytic activation. However, this strategy holds much greater potentials in generating functional epitope-directed binders to 1) block protein post-translational modifications (PTMs) beyond proteolysis, 2) block protein-protein interaction (PPI), 3) elicit agonistic or antagonistic activities on receptors, 4) stabilize protein complex, and 5) trap specific protein conformations. Our approach enables the generation of binders to the sites of interest on a wide variety of proteins for broad therapeutic and diagnostic applications.

Methods

Cloning, protein expression, and purification

Plasmids encoding wt or mutated CDCP1, MMP9, MMP1, MMP3, MMP10 and EphA2 as Fc fusions or the heavy chain and light chains of IgGs, were generated by Gibson cloning into pFUSE vector (InvivoGen). Fabs were PCR-ed from the Fab phagemid and subcloned into pBL347 Fab expression vector. Plasmids for stable cell line construction were generated by Gibson cloning into pCDH-EF1-CymR-T2A-Neo (System Bioscience) vector. Plasmid for E coli expression of MMP9-pro-cat-His^{wt} was generated by Gibson cloning into pET vector. Sequences of all plasmids were confirmed by Sanger sequencing.

Antigens for differential phage panning or antibody in IgG format were expressed by transient transfection of BirA-Expi293 cells (Life Technologies) with plasmids encoding CDCP1, MMPs and EphA2 as Fc fusion, or light/heavy chains of IgG. The ExpiFectamine 293 transfection kit (Life Technologies) was used for transfections as per manufacturer's instructions. Cells were incubated for 4-5 days at 37°C in 5% CO2 at 125 rpm before the supernatants were harvested. Proteins were purified by Protein A affinity chromatography (Fc-fusions and IgGs) and assessed for quality and integrity by SDS-PAGE.

MMP9-pro-cat-His^{wt} (E coli expression) was expressed in BL21(DE3) (Thermo Fisher). Cells were grown in 2xYT at 37°C and expression was induced with 0.5 mM isopropyl β-D-1-thiogalactopyranoside (IPTG) for 3 hours. The inclusion bodies were harvested, and the protein was refolded based on previous study.[35]

To express Fab, C43 (DE3) Pro+ E. coli transformed with the Fab expression plasmid were grown in TB autoinduction media at 37°C for 6 hrs, then switched to 30°C for 16–18 hrs.[36] Cells were harvested by centrifugation (6000xg for 20 min) and lysed with B-PER Bacterial Protein Extraction Reagent (Thermo Fischer) supplemented with DNAse I (GoldBio). Lysate was incubated at 60°C for 20 min and centrifuged at 14,000xg for 30 min. Clarified supernatant was passed through a 0.45 µm syringe filter. Fabs were purified by Protein A affinity chromatography on an AKTA Pure system. Fab purity and integrity were assessed by SDS-PAGE.

Structure bioinformatics

Secondary structures for residues in the epitope involved in binding were performed using an in-house informatics pipeline written in R. Scripts are available for download at https://github.com/crystaljie/pY_2rd_structure_solvent_accessibility_analysis.git. The antigen-Ab

complex structures used for this analysis were downloaded from AbBD.[20] DSSP algorithm was used to obtain the exact secondary structure information.[21]

Phage selection

The phage selection protocol was adapted from a previously study.[36] Briefly, selections were performed using biotinylated Fc fusion antigen captured on SA-coated magnetic beads (Promega). Prior to each selection, the phage pool was incubated with certain concentrations of biotinylated negative selection antigen captured on streptavidin beads to deplete the library of any binders to the undesired epitope. Four rounds of selection were performed with decreasing amounts of positive selection antigens (**Fig. 2b**) captured on the SA beads with soluble negative selection antigens in the solution. We employed a "catch and release" strategy, where bound Fab phage were eluted from the magnetic beads by the addition of 2 μg/mL of TEV protease. Individual phage clones from the third and fourth round of selection were analyzed for binding by phage ELISA.

Phage ELISA

Phage ELISAs were performed according to standard protocols (**Extended Data Fig. 1c**). Briefly, 384-well Maxisorp plates were coated with NeutrAvidin (10 μg/mL) overnight at 4°C and subsequently blocked with PBS + 0.2% BSA for 1 hr at 20°C. 20 nM of biotinylated positive/negative selection antigens were individually captured on the NeutrAvidin-coated wells for 30 min followed by the addition phage supernatants diluted 1:5 in PBSTB for 30 min. The "competition" wells with captured biotinylated positive selection antigen were incubated with 1:5 diluted phage in the presence of 20 nM soluble positive selection antigen. Bound phage were detected using a horseradish peroxidase (HRP)-conjugated anti-M13 phage antibody (GE Lifesciences 27-9421-01).

CDCP1 proteolysis blocking assay

Uncleaved CDCP1 ECD Fc fusion (CDCP1-Fc^{wt}) (1 μg) was treated with 0.5 μg of plasmin in 10 μL buffer for 1 hour at room temperature in the presence of IgG0151, 0152, 0153 (~ 1 μg). The samples were loaded on an SDS-PAGE gel to assess the proteolysis of CDCP1.

Mammalian Cell Culture

All the cell lines used for this study were purchased from the American Type Culture Collection (ATCC). The HEK293T or HEK293T Lenti-X cell lines was cultured in DMEM + 10% FBS + 1X Pen/Strep. MCF-7 cells were cultured in McCoy's 5A + 10% FBS + 1X Pen/Strep. The HT-1080

cell line was cultured in EMEM + 10% FBS + 1X Pen/Strep. Cell line identities were authenticated by morphological inspection. Symptoms for mycoplasma contamination were not observed and thus no test for mycoplasma contamination was performed. To the best of our knowledge, all cell lines were previously authenticated and tested for mycoplasma.

Lentiviral cell line construction

The HEK293T stable cell line overexpressing MMP9 (G100L) and HT-1080 stable cell overexpressing EphA2 were generated by lentiviral transduction. To produce virus, HEK293T Lenti-X cells were transfected with a mixture of second-generation lentiviral packaging plasmids at ~70% confluence. FuGene HD (Promega) was used for transfection of the plasmids using 3 µg DNA (1.35 µg pCMV delta8.91, 0.15 µg pMD2-G, 1.5 µg pCDH vectors encoding gene of interest) and 7.5 µL of FuGene HD per well of a six-well plate. Media was changed to complete DMEM after 6 hrs of incubation with transfection mixture. The supernatant was harvested and cleared by passing through a 0.45 µm filter 72 hrs post transfection. Cleared supernatant was added to target HEK293T or HT-1080 wt cells (~1 million cells per mL) with 8 µg/mL polybrene and cells were centrifuged at 1000xg at 33°C for 2 hrs. Cells were then incubated with viral supernatant mixture overnight before the media was changed to fresh complete DMEM. Cells were expanded for a minimum of 48 hrs before they were grown in drug selection media. Drug selection for stable cell lines was started by the addition of 2 µg/mL puromycin. Following at least 72 hrs of incubation in puromycin containing media, cells were analyzed by western blot with a MMP9 antibody (Cell Signaling Technology).

Bio-layer interferometry (BLI) experiments

BLI experiments were performed using an Octet RED384 instrument (ForteBio). Biotinylated proteins were immobilized on a streptavidin (SA) biosensor and His-tagged proteins were immobilized on a Ni-NTA biosensor. Different concentrations of analyte in PBS pH 7.4 + 0.05% Tween-20 + 0.2% BSA (PBSTB) were used as analyte. Affinities (KDs) were calculated from a global fit (1:1) of the data using the Octet RED384 software.

Western Blot

For MMP9 (G100L), conditioned medium was harvested and supplemented with protease inhibitor cocktail (Roche). After centrifuged at 14,000xg for 30 min at 4°C, the supernatant was then transferred into a new tube and protein concentration was determined by BCA assay (Bio-Rad). Immunoblotting was performed using MMP-9 (D6O3H) XP® Rabbit mAb (primary, Cell Signaling, 13667T), and IRDye 680RD Goat anti-Mouse (secondary, LiCOR, 925–68070).

Zymography analysis

Conditioned medium was harvested and then concentrated by 10 folds using a 10K cutoff spin concentrator (EMD Millipore). 4X non-reducing sample buffer (BioRad) was added to the sample, which was then loaded to the Novex™ 10% Zymogram Plus (Gelatin) Protein Gel. The gel was run at 150V until good band separation was achieved. Gel was incubated in Invitrogen Novex Zymograph renaturing buffer (Thermo Scientific) for 30 min, followed by Invitrogen Novex Zymograph developing buffer (Thermo Scientific) overnight. The gel was then stained in InstantBlue™ Coomassie Stain (Abcam) and imaged with a BioRad gel imager.

Cell migration assay

The Trans-well cell invasion assay was conducted using Costar 6.5 mm Trans-well kit (8.0 µm Pore, Corning) based per instructions. In brief, the insert was pre-coated with Matrigel (Thermo Scientific) in a 37 °C incubator for 15-30 minutes to form a thin gel layer. Cell solution (100 µL, 10^6 cells/mL, FBS free) was added on top of the Matrigel coating to simulate invasion through the extracellular matrix w/o individual inhibitory Fab (50 µg/mL). Complete medium was added to the bottom wells. Cells that migrated through the membrane were quantified using Crystal Violet (Fisher Scientific).

Cell surface protein enrichment

For the SILAC experiments, cells were cultured in DMEM SILAC media (Thermo) containing L-[13C6,15N2]lysine and L-[13C6,15N4] arginine (heavy label) (CIL) or L-[12C6,14N2]lysine and L-[12C6,14N4]arginine (light label) for seven doublings to ensure full incorporation of the isotopic labels. After 24 hr of IgG166 treatment, cells were lifted with Versene (0.04% EDTA, PBS pH 7.4 Mg/Ca free) and 20 million cells from both the heavy and light-labeled cultures were mixed at a 1:1 cell count ratio for cell surface capture and enrichment. Briefly, live cells were treated with sodium periodate buffer (2 mM NaPO4, PBS pH 6.5) at 4°C for 20 min to oxidize vicinal diols on the glycans of surface glycoproteins. Aldehydes generated by oxidation were then covalently labeled with biocytin hydrazide in a labeling buffer (PBS pH 6.5 + 1 mM biocytin hydrazide (Biotium) +10 mM aniline (Sigma)) for 90 min at 4˚C. Cells were then washed four times with PBS pH 6.5 to remove excess biocytin-hydrazide and stored overnight at −80˚C.

Frozen cell pellets were thawed and lysed in RIPA buffer (VWR) containing 1X Protease Inhibitor Cocktail (Sigma) at 4°C for 30 min. Cell lysates were sonicated, clarified, and subsequently incubated with 100 µl of NeutrAvidin Agarose (Thermo) slurry at 4°C for 30 min. The NeutrAvidin beads were then extensively washed with RIPA buffer, high salt buffer (1M NaCl, PBS pH 7.5),

and urea buffer (2M urea, 50 mM ammonium bicarbonate). Samples were reduced on-bead with 5 mM TCEP at 55°C for 30 min and alkylated with 10 mM iodoacetamide at room temperature for 30 min. To release bound proteins, proteins were subjected to on-bead digestion using 20 µg sequencing grade trypsin+LysC (Promega) at room temperature overnight. After overnight digestion, the beads were extensively washed with RIPA buffer, high salt buffer (1M NaCl, PBS pH 7.5), and urea buffer (2M urea, 50 mM ammonium bicarbonate). The eluted fraction was collected using a spin column and then desalted using ZipTips with 0.6 µL C18 resin (Millipore Sigma) following standard protocol. Desalted peptides were dried and dissolved in mass spectrometry buffer (0.1% formic acid +2% acetonitrile) prior to LC-MS/MS analysis.

Mass spectrometry analysis

1 µg of peptide was injected into a pre-packed 0.075 mm x 150 mm Acclaim Pepmap C18 LC column (2 µm pore size, Thermo Fisher) attached to a Q Exactive Plus (Thermo Fisher) mass spectrometer. Peptides were separated using a linear gradient of 3–35% solvent B (Solvent A: 0.1% formic acid, Solvent B: 80% acetonitrile, 0.1% formic acid) over 120 min at 300 µl/min. Data were collected in data-dependent acquisition mode using a top 20 method with a dynamic exclusion of 35 s and a charge exclusion restricted to charges of 2, 3, or 4. Full (MS1) scan spectrums were collected as profile data with a resolution of 140,000 (at 200 m/z), AGC target of 3E6, maximum injection time of 120 ms, and scan range of 400–1800 m/z. Fragment ion (MS2) scans were collected as centroid data with a resolution of 17,500 (at 200 m/z), AGC target of 5E4, maximum injection time of 60 ms with a normalized collision energy at 27, and an isolation window of 1.5 m/z with an isolation offset of 0.5 m/z.

Proteomics data analysis

Peptide search and MS1 peak area quantification were performed using ProteinProspector (v.5.13.2) against 20203 human proteins (Swiss-prot database, obtained March 5, 2015) with a false discovery rate of 1%. Quantitative data analysis was performed using a customized pipeline developed using R (programming language) in RStudio. To ensure stringent quantification of the surface proteome, several filters were applied to eliminate peptide identifications that we believe are due to contamination in the enrichment protocol. SILAC ratios were manually calculated from MS1 peak areas and then converted to log2 ratios normalized to a mean log2 SILAC ratio = 0 for each dataset. Median log2 SILAC ratios were calculated for each protein and p-values were calculated by a Mann-Whitney test assuming a null hypothesis of log2(SILAC Ratio) = 0

Reporting Summary

Further information on research design is available in the Nature Research Reporting Summary linked to this article.

Data availability

All data are available in the main text or the supplementary material. Any other data relating to this study are available from the corresponding authors on reasonable request.

Acknowledgements

We thank members of the Wells Lab for helpful discussion and input, in addition to members of the Recombinant Antibody Network for feedback on this project. JZ is supported by a National Institutes of Health (NIH) National Cancer Institute F32 5F32CA236151. JAW acknowledges funding from NIH NCI 1P41CA196276, CA191018, and NIH GM097316 and commercial funding from Bristol Myers Squibb.

Author contributions

JZ designed and conducted all experiments unless otherwise noted. KS and JZ conducted mass spectrometry analysis. SGR and JZ expressed MMP9 antigen in E Coli. KKL and JAW supervised the research. JZ, JAW prepared and wrote the manuscript with input from all authors.

Competing interests

The authors are preparing a provisional patent for this study.

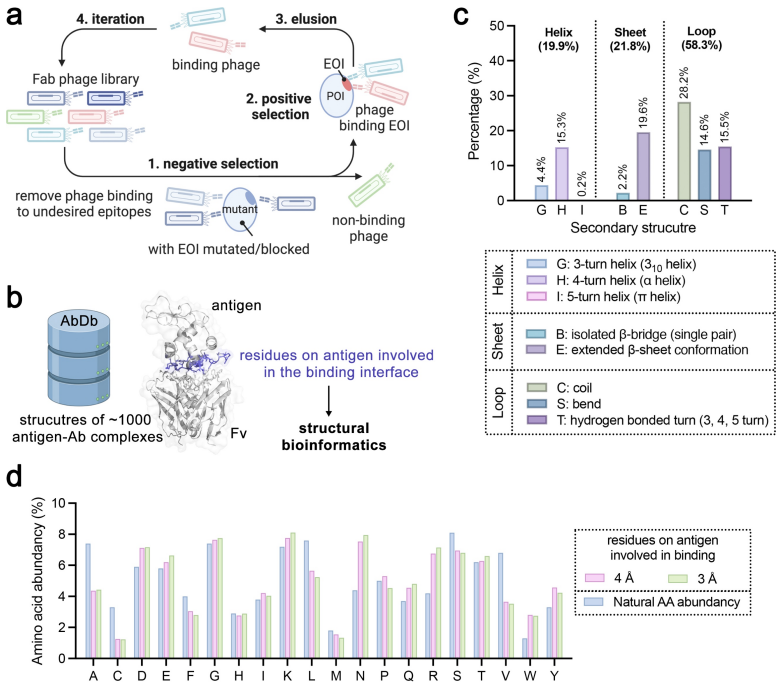

Figure 1. Strategy of epitope-directed panning against a Fab phage library. (a) Differential phage selection strategy to identify epitope-directed antibody. Fab phage library was pre-cleared with mutant with desired epitope of interest (EOI) mutated or blocked prior to positive selection with POI with desired EOI. (b) Structural bioinformatics analysis of the residues on antigens in the binding interfaces of ~1000 antigen-antibody complexes based on structures from AbDb database. Note that all the antibodies recognize a 3D epitope. (PDB: 1A2Y). (c) Antibody is more likely to bind loop regions in an antigen. The secondary structures adopted by the residues on antigens in the antigen-Ab binding interface was calculated using DSSP algorithm. (d) Abundancy of different amino acids in the epitope versus the natural amino acid abundancy. Note that 3 or 4 Å was used as distance cutoff to determine residues in the interface/epitope.

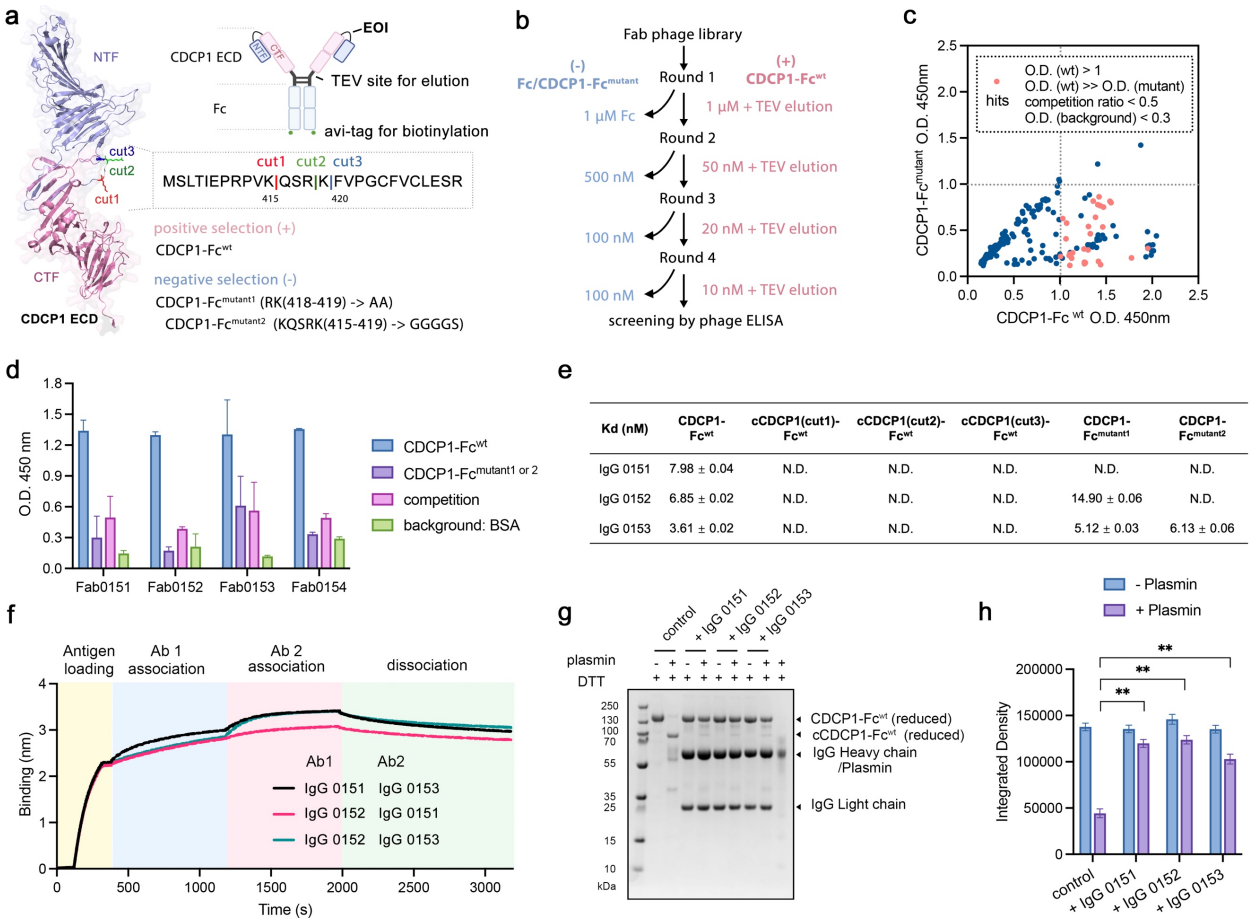

Kd (nM)	CDCP1-Fc^{wt}	cCDCP1(cut1)-Fc^{wt}	cCDCP1(cut2)-Fc^{wt}	cCDCP1(cut3)-Fc^{wt}	CDCP1-Fc^{mutant1}	CDCP1-Fc^{mutant2}
IgG 0151	7.98 ± 0.04	N.D.	N.D.	N.D.	N.D.	N.D.
IgG 0152	6.85 ± 0.02	N.D.	N.D.	N.D.	14.90 ± 0.06	N.D.
IgG 0153	3.61 ± 0.02	N.D.	N.D.	N.D.	5.12 ± 0.03	6.13 ± 0.06

Figure 2. Proof-of-concept: generating epitope-directed antibody to block CDCP1 proteolysis. (a) Design of antigens used for positive (+) and negative (-) selection for generating CDCP1 proteolysis blocking antibody. The structure of CDCP1 ECD domain was generated by AlphaFold. (b) Workflow for the differential phage selection strategy. (c) Characterization of binding of Fab phage to CDCP1-Fc^{wt} and CDCP1-Fc^{mutant} in phage ELISA revealed clones (hits) that preferentially bind CDCP1-Fc^{wt} over CDCP1-Fc^{mutant} (bottom right quadrant). Note that 96 colonies were assayed for each of the two selections cleared with CDCP1-Fc^{mutant1} and CDCP1-Fc^{mutant2} respectively. Competition ration was defined in **Extended Data Fig. 1c.** (d) As is revealed by phage ELISA, sequencing of the hits in (c), gave four unique clones, which are selective towards CDCP1-Fc^{wt} over the mutant used for negative selection. (e) In vitro binding affinities of Fab 0151 – Fab 0153 to different CDCP1 constructs: uncleaved CDCP1-Fc^{wt}, cleaved uncleaved CDCP1-Fc^{wt} with three different cut scars, and CDCP1-Fc$^{mutant1/2}$. (f) Epitope binning by BLI revealed different epitopes of IgG 0151- 0153. (g, f) SDS-PAGE gel (g) and the quantification of the band intensity revealed that the proteolysis of CDCP1 by plasmin were efficiently inhibited by the epitope-directed IgG 0151-0153.

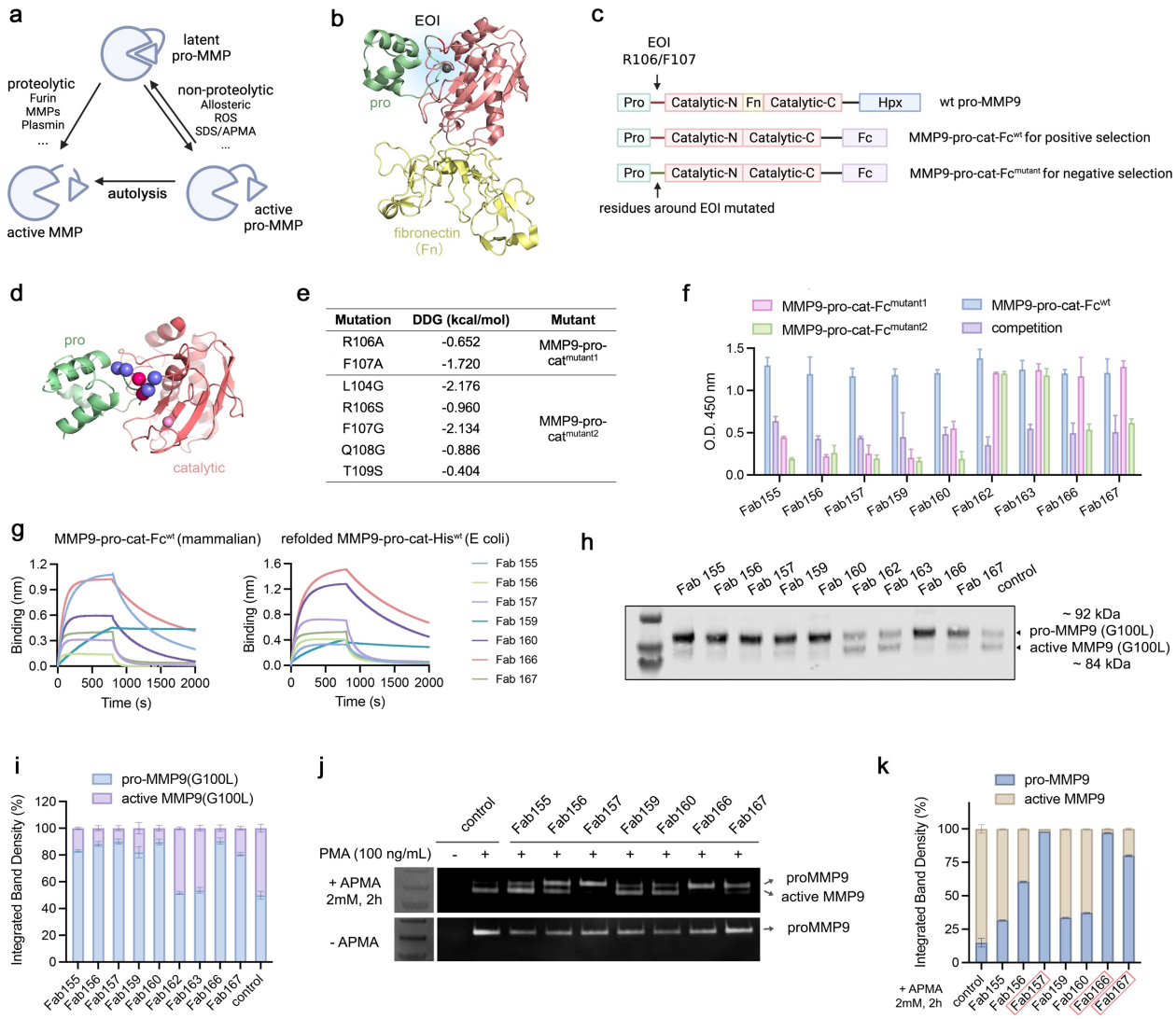

Figure 3. Generating inhibitory antibody targeting MMP9 prodomain proteolytic site to block MMP9 activation. (a) Mechanisms of proMMP activation. (b) Crystal structure of MMP9 pro-(catalytic-N)-Fn-(catalytic-C) domain. The catalytic domain of MMP9 consists of N and C-lobes with a fibronectin domain (Fn) in between. PDB: 1L6J. (c) The MMP9 constructs designed for positive and negative phage panning. The pro-catalytic domain of MMP9 was fused to a Fc with the fibronectin (Fn) and Hemopexin (Hpx) domains truncated. (d) The crystal structure of MMP9-pro-cat with mutated residues labelled in sphere. PDB: 5TH9. (e) ΔΔG values of individual mutation was calculated using INPS-MD, a web server to predict stability of protein variants from sequence and structure[27]. (f) seven out of nine unique clones enriched from phage panning selectively bind MMP9-pro-cat-Fc^{wt} over at least one of the mutants. (g) The site-directed Fabs comparably bind to mammalian expressed MMP9-pro-cat-Fc^{wt} and E coli expressed MMP9-pro-cat-His^{wt}. (h, i) Fabs block MMP9 activation. HEK293T cells stably expressing MMP9 (G100L) were treated with 25 ng/mL individual Fab overnight. The medium was harvested and subjected to SDS-PAGE. Pro and active MMP9 were visualized by WB analysis (h) using an anti-MMP9 antibody and was quantified using ImageJ (i). (j, k) Some fabs block MMP9 activation by stabilizing the interaction between prodomain and catalytic domain. The treatment of PMA (100 ng/mL, 24 hours) induced MCF-7 to express pro-MMP9. The medium was harvested and subjected to APMA (2mM, 2 hours) treatment in the presence of individual inhibitory Fabs. The pro- and active MMP9 was visualized by zymography analysis (j) and quantified using ImageJ (k).

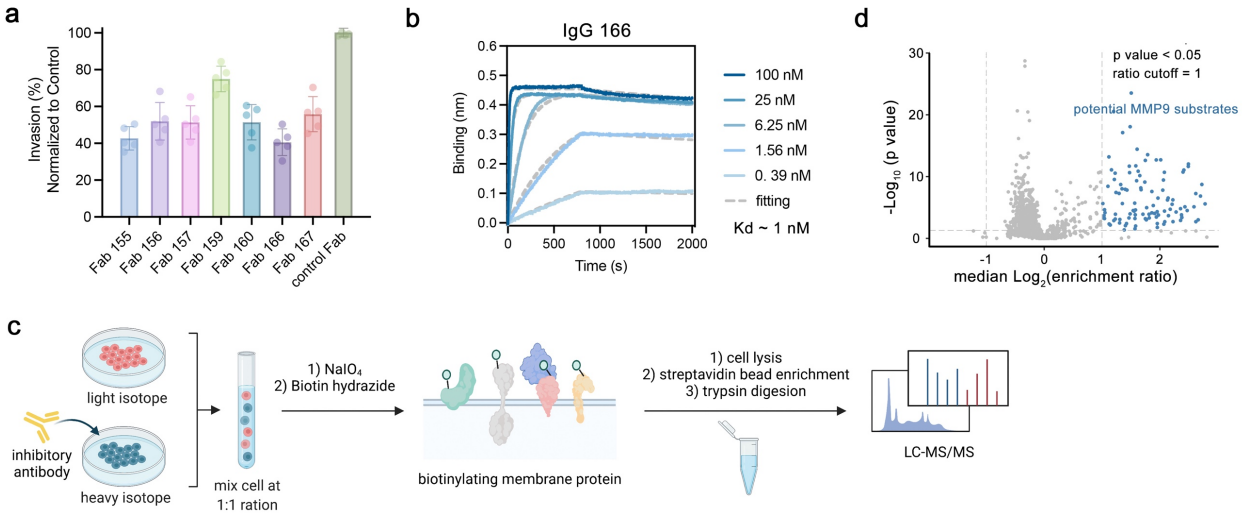

Figure 4. Potential applications of MMP9 inhibitory antibodies. (a) MMP9 inhibitory antibodies significantly slowed down HT-1080 cell invasion in a Trans-well cell invasion assay. (b) BLI characterization of Fab 166 in IgG format binding to MMP9-pro-cat-Fc^{wt}. (c) Workflow of preparation for mass spectrometry to identify potential MMP9 substrates. The concentration of IgG 166 was 50 ng/mL. (d) Volcano plot depicting proteins (blue) enriched on cells treated with IgG 166. A subset of identified proteins including known MMP9 substrates, and some potential substrates is described **in Extended Data Table 1**.

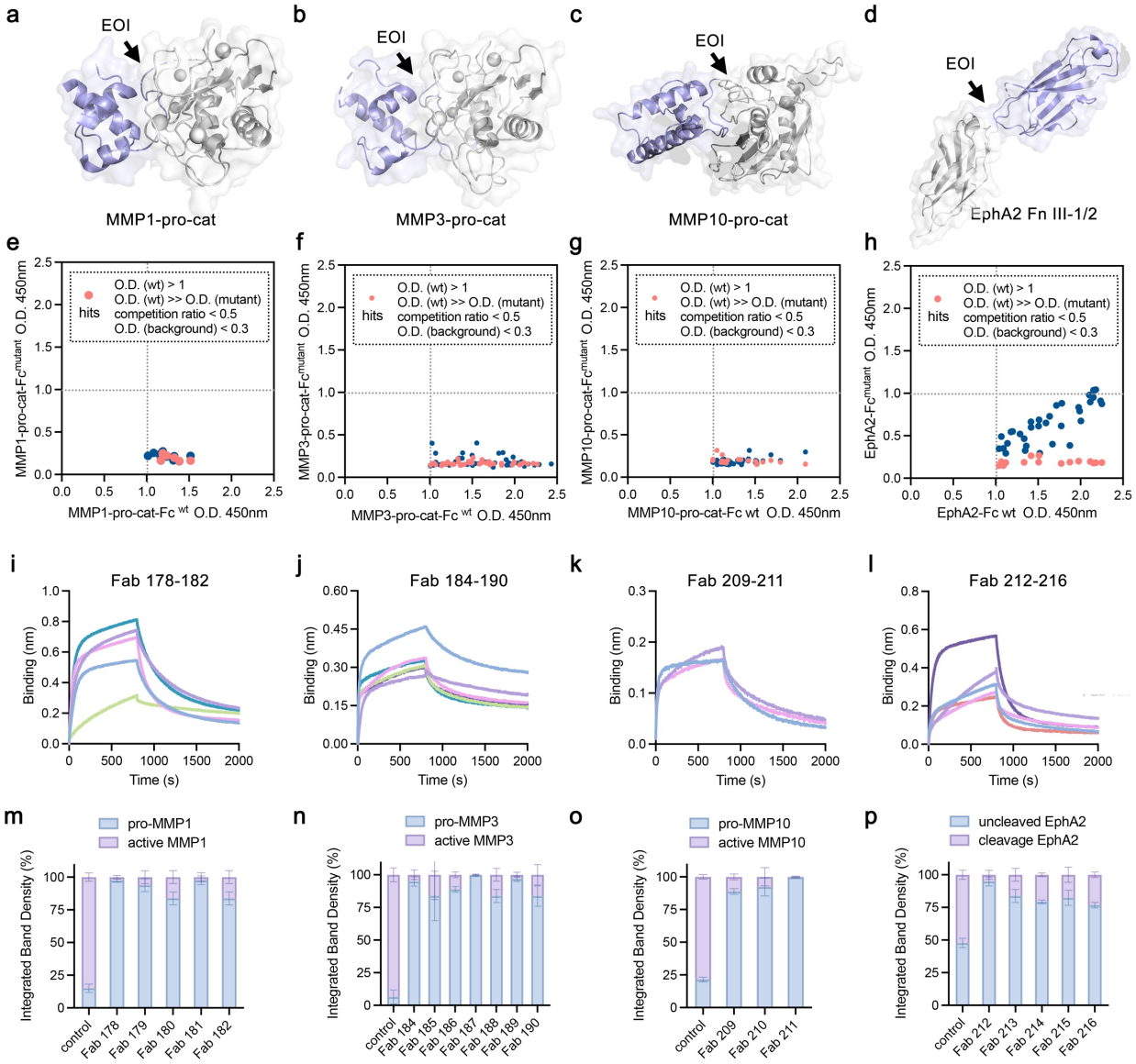

Figure 5. Generalizing differential phage selection approach to other protein targets. (a-d) Crystal or AlphaFold structures of MMP1, 3, 10 pro-catalytic domains and EphA2 Fibronectin type-III 1 and 2 domains. EOIs for proteolysis blocking purpose were indicated with an arrow. PDB: 1SU3 for MMP1, 1SLM for MMP3, AF-P09238-F1-model_v1 for MMP10, 2X10 for EphA2. (e-h) 96 clones were characterized by phage ELISA and remarkable number of clones (red) preferentially bind wt antigens over their mutants and passed through quality control. These fab phages were Sanger sequenced to get unique sequences. (i-l) BLI characterization of unique clones from each selection campaign in Fab format binding to wt antigens. These Fabs have minimum binding to corresponding mutants shown in **Extended Data Fig. 10**. (m-o) proMMP activation of MMP1, MMP3 and MMP10 was inhibited by different Fabs. ProMMPs and active MMPs were visualized by SDS-PAGE and Quantification was conducted ImageJ. (p) EphA2 proteolysis in HT-1080 stable cell line was inhibited by different blocking antibodies. The proteolysis of EphA2 was monitored by western blot and quantified by ImageJ.

Reference

1 Weiner, L. M., Surana, R. & Wang, S. Z. Monoclonal antibodies: versatile platforms for cancer immunotherapy. *Nature Reviews Immunology* **10**, 317-327, doi:10.1038/nri2744 (2010).

2 Mahoney, K. M., Rennert, P. D. & Freeman, G. J. Combination cancer immunotherapy and new immunomodulatory targets. *Nature Reviews Drug Discovery* **14**, 561-584, doi:10.1038/nrd4591 (2015).

3 Topalian, S. L., Taube, J. M., Anders, R. A. & Pardoll, D. M. Mechanism-driven biomarkers to guide immune checkpoint blockade in cancer therapy. *Nature Reviews Cancer* **16**, 275-287, doi:10.1038/nrc.2016.36 (2016).

4 Waldmann, T. A. & O'Shea, J. The use of antibodies against the IL-2 receptor in transplantation. *Current Opinion in Immunology* **10**, 507-512, doi:10.1016/s0952-7915(98)80215-x (1998).

5 Green, L. Transgenic mouse strains as platforms for the successful discovery and development of human therapeutic monoclonal antibodies. *Current drug discovery technologies* **11 1**, 74-84 (2014).

6 Winter, G., Griffiths, A. D., Hawkins, R. E. & Hoogenboom, H. R. Making antibodies by phage display technology *Annual Review of Immunology* **12**, 433-455, doi:10.1146/annurev.iy.12.040194.002245 (1994).

7 Gai, S. A. & Wittrup, K. D. Yeast surface display for protein engineering and characterization. *Current Opinion in Structural Biology* **17**, 467-473, doi:10.1016/j.sbi.2007.08.012 (2007).

8 Chen, L. X. *et al.* Epitope-directed antibody selection by site-specific photocrosslinking. *Science Advances* **6**, doi:10.1126/sciadv.aaz7825 (2020).

9 Gao, J., Sidhu, S. S. & Wells, J. A. Two-state selection of conformation-specific antibodies. *Proceedings of the National Academy of Sciences of the United States of America* **106**, 3071-3076, doi:10.1073/pnas.0812952106 (2009).

10 Lim, S. A. *et al.* Targeting a proteolytic neo-epitope of CUB-domain containing protein 1 in RAS-driven cancer. *bioRxiv*, 2021.2006.2014.448427, doi:10.1101/2021.06.14.448427 (2021).

11 Hill, Z. B., Martinko, A. J., Nguyen, D. P. & Wells, J. A. Human antibody-based chemically induced dimerizers for cell therapeutic applications. *Nature Chemical Biology* **14**, 112-+, doi:10.1038/nchembio.2529 (2018).

12 Werb, Z. ECM and cell surface proteolysis: Regulating cellular ecology. *Cell* **91**, 439-442, doi:10.1016/s0092-8674(00)80429-8 (1997).

13 Kessenbrock, K., Plaks, V. & Werb, Z. Matrix Metalloproteinases: Regulators of the Tumor Microenvironment. *Cell* **141**, 52-67, doi:10.1016/j.cell.2010.03.015 (2010).

14 Sato, H. *et al.* A Matrix Metalloproteinase Expressed On The Surface Of Invasive Tumor-Cells. *Nature* **370**, 61-65, doi:10.1038/370061a0 (1994).

15 Yan, R. Q. *et al.* Membrane-anchored aspartyl protease with Alzheimer's disease beta-secretase activity. *Nature* **402**, 533-537, doi:10.1038/990107 (1999).

16 Vassar, R. *et al.* beta-secretase cleavage of Alzheimer's amyloid precursor protein by the transmembrane aspartic protease BACE. *Science* **286**, 735-741, doi:10.1126/science.286.5440.735 (1999).
17 Tedgui, A. & Mallat, Z. Cytokines in atherosclerosis: Pathogenic and regulatory pathways. *Physiological Reviews* **86**, 515-581, doi:10.1152/physrev.00024.2005 (2006).
18 Friedl, P. & Alexander, S. Cancer Invasion and the Microenvironment: Plasticity and Reciprocity. *Cell* **147**, 992-1009, doi:10.1016/j.cell.2011.11.016 (2011).
19 Friedl, P. & Wolf, K. Tumour-cell invasion and migration: Diversity and escape mechanisms. *Nature Reviews Cancer* **3**, 362-374, doi:10.1038/nrc1075 (2003).
20 Ferdous, S. & Martin, A. C. R. AbDb: antibody structure database-a database of PDB-derived antibody structures. *Database-the Journal of Biological Databases and Curation*, doi:10.1093/database/bay040 (2018).
21 Kabsch, W. & Sander, C. DICTIONARY OF PROTEIN SECONDARY STRUCTURE - PATTERN-RECOGNITION OF HYDROGEN-BONDED AND GEOMETRICAL FEATURES. *Biopolymers* **22**, 2577-2637, doi:10.1002/bip.360221211 (1983).
22 Ikeda, J. I. *et al.* Expression of CUB domain containing protein (CDCP1) is correlated with prognosis and survival of patients with adenocarcinoma of lung. *Cancer Science* **100**, 429-433, doi:10.1111/j.1349-7006.2008.01066.x (2009).
23 Scherl-Mostageer, M. *et al.* Identification of a novel gene, CDCP1, overexpressed in human colorectal cancer. *Oncogene* **20**, 4402-4408, doi:10.1038/sj.onc.1204566 (2001).
24 Casar, B. *et al.* Blocking of CDCP1 cleavage in vivo prevents Akt-dependent survival and inhibits metastatic colonization through PARP1-mediated apoptosis of cancer cells. *Oncogene* **31**, 3924-3938, doi:10.1038/onc.2011.555 (2012).
25 Vandooren, J., Van den Steen, P. E. & Opdenakker, G. Biochemistry and molecular biology of gelatinase B or matrix metalloproteinase-9 (MMP-9): The next decade. *Critical Reviews in Biochemistry and Molecular Biology* **48**, 222-272, doi:10.3109/10409238.2013.770819 (2013).
26 Ra, H.-J. & Parks, W. C. Control of matrix metalloproteinase catalytic activity. *Matrix Biology* **26**, 587-596, doi:https://doi.org/10.1016/j.matbio.2007.07.001 (2007).
27 Savojardo, C., Fariselli, P., Martelli, P. L. & Casadio, R. INPS-MD: a web server to predict stability of protein variants from sequence and structure. *Bioinformatics* **32**, 2542-2544, doi:10.1093/bioinformatics/btw192 (2016).
28 Fisher, K. E. *et al.* Engineering autoactivating forms of matrix metalloproteinase-9 and expression of the active enzyme in cultured cells and transgenic mouse brain. *Biochemistry* **41**, 8289-8297, doi:10.1021/bi012076t (2002).
29 Shin, Y. H. *et al.* PMA-induced up-regulation of MMP-9 is regulated by a PKCα-NF-κB cascade in human lung epithelial cells. *Experimental & Molecular Medicine* **39**, 97-105, doi:10.1038/emm.2007.11 (2007).
30 Itoh, T. *et al.* Experimental metastasis is suppressed in MMP-9-deficient mice. *Clinical & Experimental Metastasis* **17**, 177-181, doi:10.1023/a:1006603723759 (1999).
31 Apweiler, R., Hermjakob, H. & Sharon, N. On the frequency of protein glycosylation, as deduced from analysis of the SWISS-PROT database. *Biochimica Et Biophysica Acta-General Subjects* **1473**, 4-8, doi:10.1016/s0304-4165(99)00165-8 (1999).

32 Wollscheid, B. *et al.* Mass-spectrometric identification and relative quantification of N-linked cell surface glycoproteins. *Nature Biotechnology* **27**, 378-386, doi:10.1038/nbt.1532 (2009).

33 Xu, D. M. *et al.* Novel MMP-9 Substrates in Cancer Cells Revealed by a Label-free Quantitative Proteomics Approach. *Molecular & Cellular Proteomics* **7**, 2215-2228, doi:10.1074/mcp.M800095-MCP200 (2008).

34 Koshikawa, N. *et al.* Proteolysis of EphA2 Converts It from a Tumor Suppressor to an Oncoprotein. *Cancer Research* **75**, 3327-3339, doi:10.1158/0008-5472.Can-14-2798 (2015).

35 Appleby, T. C. *et al.* Biochemical characterization and structure determination of a potent, selective antibody inhibitor of human MMP9. *Journal of Biological Chemistry* **292**, 6810-6820, doi:10.1074/jbc.M116.760579 (2017).

36 Hornsby, M. *et al.* A High Through-put Platform for Recombinant Antibodies to Folded Proteins. *Molecular & Cellular Proteomics* **14**, 2833-2847, doi:10.1074/mcp.O115.052209 (2015).